Solar-Terrestrial Physics. 2019. Vol. 5. Iss. 4. P. 3–9. DOI: 10.12737/stp-54201901. © 2019 A.V. Borovik, A.A. Zhdanov. Published by INFRA-M Academic Publishing House
Original Russian version: A.V. Borovik, A.A. Zhdanov, published in Solnechno-zemnaya fizika. 2019. Vol. 5. Iss. 4. P. 3–11. DOI: 10.12737/szf-54201901. © 2019 INFRA-M Academic Publishing House (Nauchno-Izdatelskii Tsentr INFRA-M)

PROCESSES OF ENERGY RELEASE IN LOW-POWER SOLAR FLARES

A.V. Borovik
Institute of Solar-Terrestrial Physics SB RAS, Irkutsk, Russia, aborovik@iszf.irk.ru

A.A. Zhdanov
Institute of Solar-Terrestrial Physics SB RAS, Irkutsk, Russia, kick.out@mail.ru

Abstract. Using flare patrol data for 1972–2010 [http://www.ngdc.noaa.gov/stp/space-weather/solar-data/solar-features/solar-flares/], we have conducted statistical studies of small solar flares. We have established a correlation between the flare brightness rise time and the total duration of small flares, and obtained evidence of the discreteness of relative rise times (T_{rel}). The most significant T_{rel} values are 0.2, 0.25, 0.33, and 0.5. As the area class and importance of flares increase, maxima of T_{rel} distributions decrease, flatten, and completely disappear in case of large flares. We have found the discreteness of the area distribution of small flares. We have obtained distributions of solar flare energy, which exhibit significant overlap for flare energy of different area classes. The energy range of large solar flares contains 9.5 % of small flares. The energy range of flares of area class 1 has even a more significant overlap.

Keywords: solar flares.

INTRODUCTION

Solar flares — phenomenon of rapid transformation of energy of plasma electric currents into energy of powerful hydrodynamic motions, heat fluxes, particle emission and acceleration — generate a complex chain of processes affecting Earth's magnetosphere, ionosphere, and neutral atmosphere, have a significant effect on the radiation situation in near-Earth space.

Observations in a wide range of wavelengths demonstrate that solar flares are driven by large-scale reconnection of coronal magnetic fields. In the region of contact between oppositely directed magnetic fluxes, current sheets are formed. During their break followed by a magnetic reconnection, the excess energy is converted into kinetic energy of accelerated particles and thermal energy of plasma [Priest, 1992; Rust, Gauzzi, 1992; Somov, 1992; Roumeliotis, Moore, 1993; Masuda et al, 1994.; Raman et al., 1994]. The energetic particles propagating along magnetic field lines into the chromosphere generate optical and hard X-rays in footpoints of the field lines. Heated to high temperatures, the chromospheric plasma evaporates, fills magnetic loops, and becomes visible in UV and soft X-rays. A relationship has been found between hard and soft X-ray fluxes in solar flares: time derivative of the soft X-ray flux is proportional to the hard X-ray flux (Neupert effect) [Neupert, 1968]. As for the optical emission of solar flares, especially during their initial phase, we cannot yet draw definitive conclusions — the physical picture is too complex [Somov, 1992; Fletcher et al., 2011]. Attempts to find a relationship between optical parameters of flares yielded no results [Smith, Smith, 1966]. No relationship was found between flare duration, area, intensity and Hα line width. The correlation between maximum Hα line width and flare importance is rather low. There is no relationship between the time of brightness rise to maximum and the time of its decay (according to our estimates, the correlation coefficient is less than 0.4).

Borovik, Zhdanov [2017b, 2018a, 2018b] using a great body of data have obtained distributions of solar flares by the time of brightness rise to maximum, decay time, and total duration in accordance with the international classification of chromospheric flares. According to the optical classification, flares are divided by area into five classes: S, 1, 2, 3, 4. In each class of area, flares are subdivided into three classes of brightness: F (faint flares), N (normal), and B (bright). The combination of these two parameters constitutes the optical importance of flare.

In this paper, we analyze the results obtained in [Borovik, Zhdanov, 2017b, 2018a, 2018b], present a number of important, in our opinion, conclusions about dynamics and power of flare processes.

RESULTS

1. Correlation relationships between optical parameters of solar flares

We have carried out statistical studies, using international flare patrol data for 1972–2010 [http://www.ngdc.noaa.gov/stp/space-weather/solar-data/solar-features/solar-flares/]. We have separately performed studies, using data from Holloman Solar Observatory (HOLL, New Mexico, USA), Learmonth Solar Observatory (LEAR, Australia), and Ramey Solar Observatory (RAMY, Puerto Rico), which employ identical automated vacuum 25-cm refractors equipped with tunable monochromatic filters, centered to the Hα line (spatial resolution of the telescope is ~0.3 arcsec). During the observations, flare intensity, time of emission increase and decrease are determined automatically, the chromosphere area covered by the emission is calculated and corrected for foreshortening. A flare of 160–260 % brightness relative to the bright-

ness of the quiet chromosphere are considered faint (F); of 260–360 %, normal (N); over 360%, bright (B).

Our analysis has established that for small S-class solar flares (area less than 194 m.s.d.) there is a high correlation between the total flare duration and the brightness rise time. The correlation coefficient $r \approx 0.7$ (Table 1). For large flares of classes 2–4 whose area exceeds 504 m.s.d., $r \approx 0.5$.

Table 1

Correlation coefficients: rise–duration

	All flares		HOLL, LEAR, RAMY	
	N	*r*	*N*	*r*
SF	59555	0.69	34083	0.69
SN	20202	0.64	6194	0.63
SB	4226	0.63	2127	0.62
1F	2453	0.66	1049	0.63
1N	3423	0.65	1144	0.65
1B	1775	0.59	835	0.61
(2–4)F	168	0.31	71	0.58
(2–4)N	467	0.66	162	0.47
(2–4)B	653	0.55	371	0.53
S	83983	0.67	42404	0.67
1	7651	0.63	3028	0.63
2–4	1288	0.56	604	0.52

A similar conclusion is drawn from the analysis of flares of certain types (Table 2). The highest correlation coefficient (0.7–0.8) is exhibited by H-type flares accompanied by high-speed filament ejection.

Table 2

Correlation coefficients between brightness rise time and total duration of flares of certain types

Type	Class S		Class 1		Class 2–4	
V	2762	0.61	271	0.65	50	0.46
K	1029	0.51	309	0.56	97	0.61
H	2357	0.78	434	0.74	128	0.79
U	569	0.59	432	0.65	232	0.59
G	484	0.63	68	0.79	6	0.43
D	3291	0.69	218	0.70	31	0.48
E	6859	0.68	1501	0.66	233	0.48

Notes: *N* – number of flares; *r* – correlation coefficient;
V – considerable expansion for about 1 min that often includes a significant intensity increase (explosive flare);
K – several intensity maxima;
H – flare accompanied by high-speed dark filament;
U – two bright branches, parallel or converging (two-ribbon flare);
G – no visible spots nearby (spotless flare);
D – brilliant point;
E – two or more brilliant points;

This relationship initiated a more detailed analysis of the relative brightness rise time (T_{rel} — a parameter representing the ratio of the brightness rise time to the total flare duration) using a large number of events.

2. Relative brightness rise times of solar flares

Reports from stations about the same flare usually differ, and in catalogs flares are grouped together under one number [Solar-Geophys. Data, 1983]. To estimate the variance of T_{rel}, in the group reports from stations for area classes and importance of flares we have determined mean standard deviations of T_{rel} ($\overline{\sigma}$). According to the results, with increasing area class and importance $\overline{\sigma}$ gradually decreases from 0.12 to 0.08 (Table 3).

Table 3

$\overline{\sigma}T_{rel}$ as a function of class and importance of flares. N_{gr} is the number of grouped analyzed

	N_{gr}	$\overline{\sigma}$
SF	6417	0.12
SN	2600	0.11
SB	599	0.09
1F	155	0.09
1N	466	0.10
1B	375	0.08
(2–4)F	12	0.08
(2–4)N	65	0.08
(2–4)B	157	0.09
S	13386	0.12
1	1646	0.09
2–4	353	0.09

We have statistically analyzed T_{rel} for 73416 flares. We obtained distributions of T_{rel} for flares of certain classes and importance. Statistical parameters of the distributions are listed in Table 4, which shows the number of flares *N*, mean relative brightness rise time $\overline{T}_{rel}$ with a confidence interval α, median distributions *Me*, intervals T_{rel} for 90 % of flares ΔT_{rel}.

For small flares $\overline{T}_{rel} \sim 0.28$, $Me \sim 0.25$. For 90 % of small flares ΔT_{rel} does not exceed 0.54. By comparison, according to [Smith, Smith, 1966] the mean relative brightness rise time for small flares is 0.36; class 1 flares, 0.28; large flares, 0.24.

The parameter changes indicate that the ratio of rise time to total duration of flares with increasing area class, importance, and brightness gradually decreases (Figure 1, Table 4).

According to the HOLL, LEAR and RAMY data we processed, mean relative brightness rise times of small flares differ slightly (Figure 2, *a*). In flares of higher area classes, they differ within the scattering range $\overline{\sigma}$.

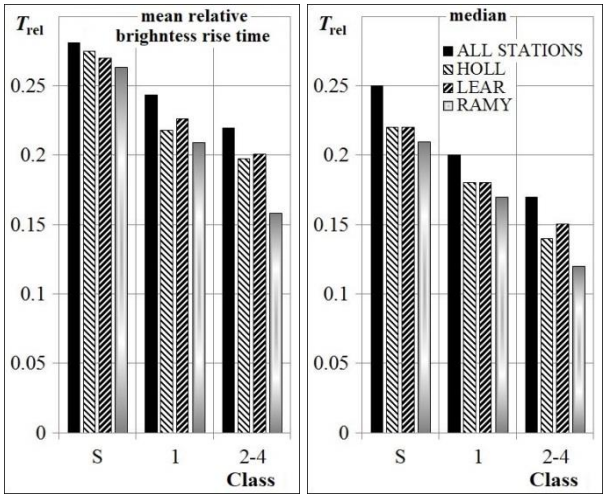

Figure 1. Change in statistical parameters of T_{rel} distributions with increasing area class of flares as derived from flare patrol, HOLL, LEAR, and RAMY data

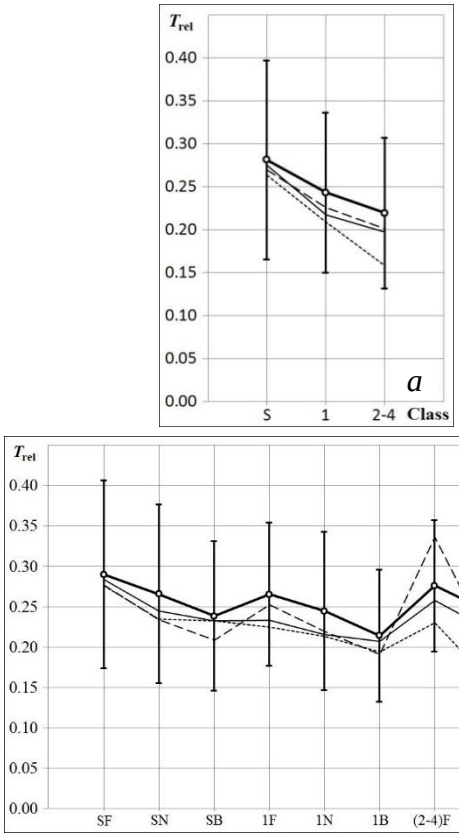

Figure 2. Change in $\overline{T}_{rel}$ with increasing area class (*a*) and importance of flares (*b*) according to data from HOLL, LEAR, RAMY, and all stations. Scattering ranges $\overline{\sigma}$ are indicated by vertical lines

More significant differences are observed for importance of flares (Figure 2, *b*). This may be due to the insufficient quality of statistical weight of data, especially for large flares. Nevertheless, there is a good tendency of the relative brightness rise time with increasing importance.

All the T_{rel} distributions have a positive asymmetry and an extended decrease and, like time parameters of flares [Borovik, Zhdanov, 2017b, 2018a, 2018b], exhibit a significant mutual overlap of distributions (Figure 3, *a*, *b*). This implies that the high percentage of flares with increasing area class does not show the general tendency.

Also noteworthy is the presence of a number of maxima (Figures 4, 5) in the distributions of small flares, with the most significant being 0.2, 0.25, 0.33, and 0.5. With increasing area classe3+s and importance, the maxima decrease, flatten, and almost completely disappear in case of large flares.

As additional evidence for the possible discreetness of T_{rel} of small flares, Figure 6 shows T_{rel} distributions for solar flares of 7 types.

There are distinct maxima of T_{rel} in distributions of D- and G-flares. In the distributions of V-, H- and E-flares, maxima gradually decrease and disappear in U- and K-flares.

Small explosive flares and two-ribbon flares have the shortest mean relative brightness rise times. The mean relative brightness rise time for D- and G-flares is longer than that for flares of other types (Table 5, Figure 7).

Table 4

Statistical parameters of T_{rel} distributions for importance, area classes, and brightness of solar flares

	N	$\overline{T}_{отн} \pm \alpha$	*Me*	ΔT_{rel} (90 %)
SF	46277	0.29±0.002	0.25	0.54
SN	16258	0.27±0.003	0.23	0.50
SB	3440	0.24±0.006	0.20	0.47
1F	1859	0.27±0.007	0.23	0.50
1N	2794	0.24±0.006	0.20	0.46
1B	1531	0.21±0.008	0.17	0.43
(2–4)F	156	0.28±0.027	0.25	0.50
(2–4)N	444	0.24±0.015	0.20	0.48
(2–4)B	657	0.19±0.011	0.14	0.39
S	65974	0.28±0.001	0.25	0.52
1	6184	0.24±0.004	0.20	0.46
2–4	1257	0.22±0.009	0.17	0.44
F	48292	0.29±0.002	0.25	0.54
N	19496	0.26±0.002	0.22	0.50
B	5628	0.23±0.004	0.18	0.45

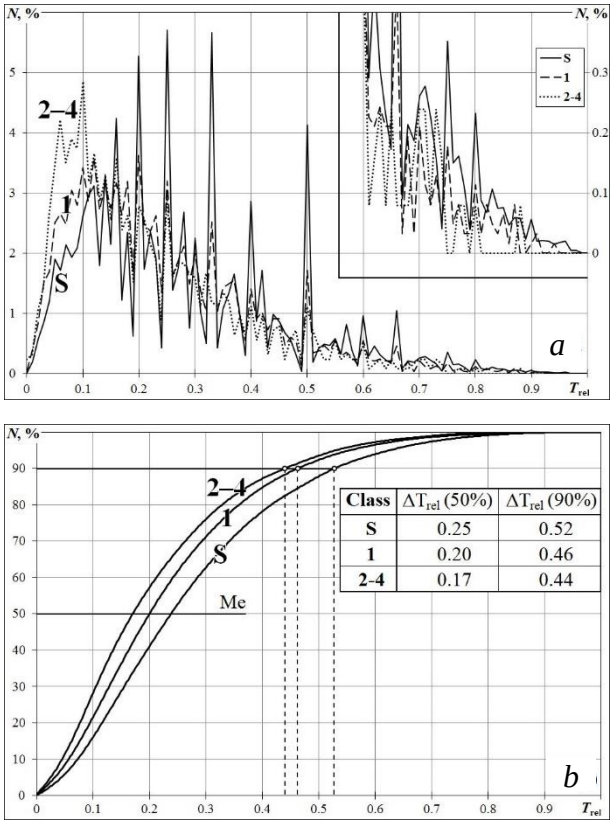

Figure 3. Distribution of the relative brightness rise time of class S, 1, and 2–4 flares (*a*) (solid line shows class S flares; dashed line, class 1 flares; dotted line, class 2–4 flares). Distribution tails are scaled up (right axis); cumulative frequency plots (*b*). Table lists intervals of T_{rel} for 50 and 90 % of flares

Note that neither the distribution by brightness rise time of flares nor the distribution by their total duration are discrete [Borovik, Zhdanov, 2018a, 2018b]. The maxima are likely to de unrelated with the observation time discreteness — spread of time parameters of flares within the maxima is quite significant. Nevertheless, this result requires further careful study. We do not exclude that the discreetness of T_{rel} of small flares can be a real phenomenon.

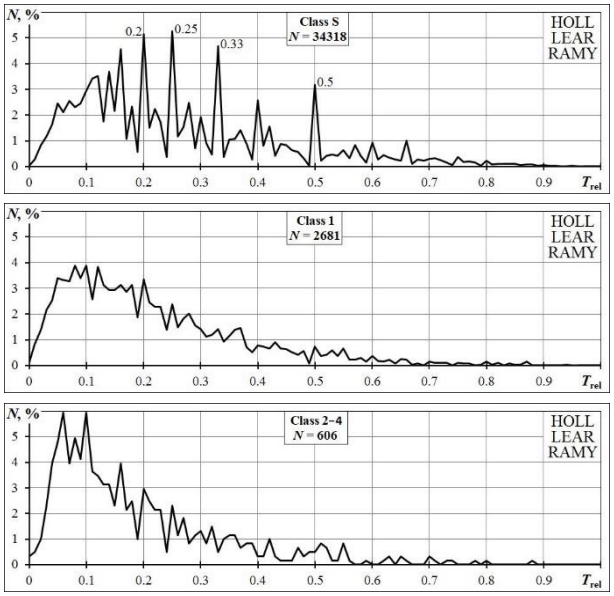

Figure 4. Distribution of the relative brightness rise time for solar flares of area classes S, 1, 2–4 as derived from HOLL, LEAR, and RAMY data within 65° from the central meridian

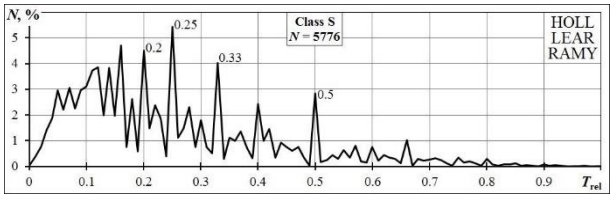

Figure 5. Distribution of the relative brightness rise time of class S solar flares within 10° from the central meridian

3. Structural features of small solar flares

According to current model representations, small solar flares are assigned to the structures of simple-loop type. In soft X-rays, it has small volumes, low heights, and high energy densities. Energy of loop flare is usually released during the impulsive phase. The most typical is one burst of hard X-rays lasting about a minute [Priest, 1985].

According to observations in the Hα line on the solar disk, small flares are small bright knots that are not always connected to each other and do not always form ribbons. On the limb, small flares occur as bright spots, which then rapidly form a single radiation source being usually conical or cylindrical in shape. Over time, they may expand, pulsate, produce ejections and loops [Severnyi, Shaposhnikova, 1961; Smith, Smith, 1966; Ogir', 1970; Švestka, 1976].

Borovik [1994] has found that small flares have a discrete structure and consist of three basic elements: flare knot, cluster, and loop. The flare knot has an elongated ellipsoidal shape, the characteristic dimension of flare knots is 1.5×3 arcsec, and the area is ~1.2 m.s.d. They often form a dense cluster. During the initial phase of development, the cluster looks like a big bright knot from which loops radiate. At the decay phase, it is usually resolved into separate knots connected by loops, which are a link between the flare knots. One of the footpoints is often brighter than the other. Single flare knots produce weak loops closed upon nodes of enhanced chromospheric network. The characteristic dimensions

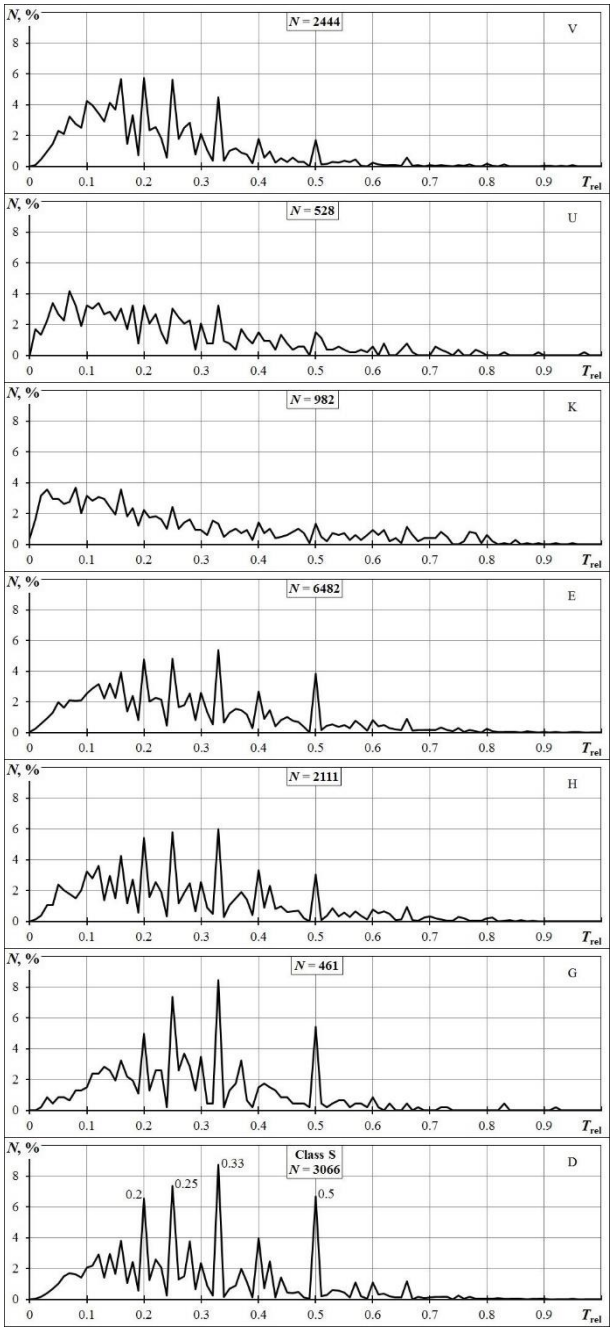

Figure 6. Distributions of relative brightness rise times for low-power flares of seven types within 65° from the central meridian

of the loops are 10 and 30 thousand kilometers. Small flares usually emerge and develop along boundaries of convective cells of mesogranule and supergranule types, often forming ring-shaped structures [Borovik, 1990].

On the limb, a small flare appears as one or two adjacent cones, the distance between which is from 7 to 37 thousand kilometers. As the flare develops, there may appear loops between the cones. A careful study of the inside of the flare cone can reveal one or two narrow elongated bright features — jet-type structures. If the cone contains two jets, they tend to converge at the vertex of the cone and eventually stretch upward. Limb small flares often have a fairly complex structure consisting of a system of knots and loops.

Table 5

Statistical parameters of T_{rel} distributions for flares of certain types

Type	Class S				Class 1				Class 2–4			
	N	$\overline{T}_{отн} \pm \alpha$	*Me*	$\Delta T_{отн}$ (90 %)	*N*	$\overline{T}_{отн} \pm \alpha$	*Me*	$\Delta T_{отн}$ (90 %)	*N*	$\overline{T}_{отн} \pm \alpha$	*Me*	$\Delta T_{отн}$ (90 %)
V	2444	0.23±0.006	0.20	0.40	260	0.18±0.015	0.15	0.35	50	0.16±0.041	0.10	0.36
U	528	0.24±0.015	0.20	0.50	425	0.20±0.014	0.17	0.40	225	0.18±0.016	0.14	0.34
K	982	0.26±0.013	0.19	0.61	304	0.27±0.022	0.22	0.56	97	0.26±0.036	0.22	0.52
E	6482	0.28±0.004	0.25	0.50	1478	0.24±0.008	0.20	0.48	228	0.23±0.021	0.18	0.49
H	2111	0.28±0.007	0.25	0.50	420	0.24±0.014	0.21	0.45	126	0.22±0.029	0.16	0.48
G	461	0.29±0.014	0.26	0.50	68	0.25±0.028	0.23	0.38	6	0.24±0.070	0.25	0.33
D	3066	0.29±0.006	0.26	0.50	212	0.28±0.022	0.23	0.50	30	0.22±0.061	0.15	0.36

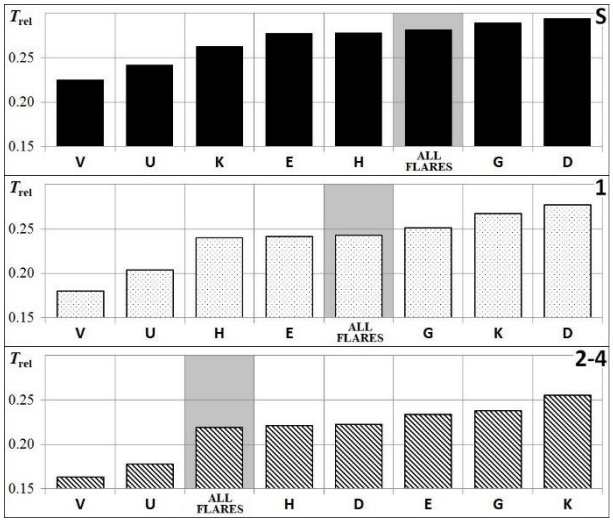

Figure 7. Mean relative brightness rise time for flares of certain types as a function of area class. Histograms are plotted in the order of increasing T_{rel}

Due to the peculiarities of the development and structure of small flares, their distribution in area exhibit, unlike large flares, a well-defined maximum of 21 m.s.d. (Figure 8, Table 6).

A more detailed study based on data from HOLL, LEAR, RAMY, the resolution of telescopes of which exceeds several times the size of the fine structure of small flares, has found that the distribution includes at least two maxima: 15 and 21 m.s.d. (Figure 9). According to our estimates, they may be related to flares developing along mesogranule boundaries.

Table 6

Statistical parameters of distributions of flares by area

	N	$\overline{S} \pm \alpha$	*Mo*	*Me*	ΔS (90 %)
SF	49305	49.8±0.3	21	38	1–101
SN	15927	84.5±0.7	31	76	5–154
SB	3456	100.9±1.6	64	96	10–174
1F	1296	271.7±3.8	–	249	200–383
1N	2340	285.4±2.9	–	266	200–403
1B	1586	305.4±4.0	–	287	200–436
(2–4)F	65	750.2±91.2	–	620	500–1045
(2–4)N	281	421.3±32.1	–	627	500–1047
(2–4)B	504	812.1±33.7	–	675	500–1211
S	68688	60.4±0.3	21	46	1–126
1	5222	28.1±2.1	–	266	200–410
2–4	850	777.3±23.8	–	654	500–1110

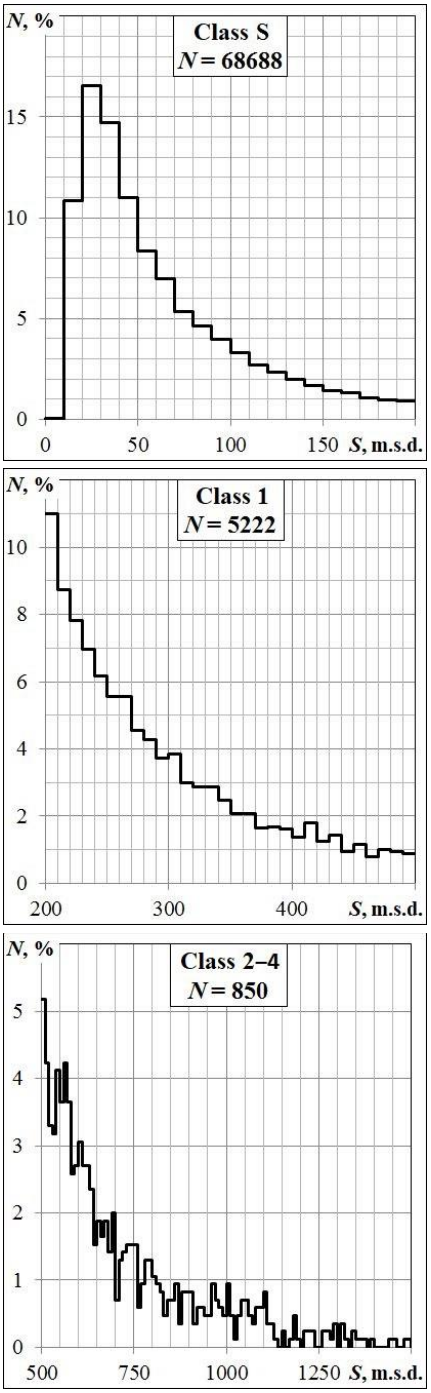

Figure 8. Area distribution of solar flares in terms of foreshortening within 65° from the central meridian

4. Energy of solar flares

One of the fundamental questions of solar flare physics is the mechanism of energy accumulation and release. According to the statistics [Borovik, Zhdanov, 2017a], on the Sun there are more than 90 % of small flares with energy $\approx 10^{29}$ erg and approximately 1.5 % of large flares, the energy of the most powerful of which is $\approx 3 \cdot 10^{32}$ erg. Most energy of the flares is in the ultraviolet region and Balmer lines [Woods et al., 2006]. The papers [Kurochka, Stasjuk, 1981; Kurochka, Rossada, 1981a, 1981b] have demonstrated that the total energy of flares in all lines and continua of hydrogen series is closely related to the emission in the Hα line. Taking into account the time variation of area and intensity of flares, the authors have derived an expression for the total mean energy emitted by optical flares of different power (Table 7, Column II).

$$E = 4.7 \cdot 10^{-22}\, \alpha(i)\, \mathrm{S}(i)\, T(i)\, I^2(i),$$

where E is the flare energy, erg; i is the flare importance; $I(i)$ is the Hα central intensity, erg/(cm^3·s·sr); S(i) is the typical area of flare, cm^2; $T(i)$ is the typical lifetime of flare s; α(i) is the coefficient taking into account the intensity distribution in flare.

Using data on α(i) and $I(i)$ from [Kurochka, Stasjuk, 1981; Kurochka, Rossada, 1981a, 1981b] and distributions of flares by duration [Borovik, Zhdanov, 2018a] and area, we have obtained distributions of solar flares by energy in the visible spectrum depending on area class and importance (Figure 10). The results have revealed slight differences in mean energies of flares (Table 7).

Table 7

Mean energies of flares n the visible spectrum

	N	$\bar{S} \cdot 10^{-18}$, см^2		$\bar{T} \cdot 10^{-3}$, с		$\bar{E}$, эрг	
		I	II	I	II	I	II
SF	49305	0.8	1.7	1.1	1.0	$2.2 \cdot 10^{27}$	$3.8 \cdot 10^{27}$
SN	15927	1.3	1.7	1.4	1.0	$8.7 \cdot 10^{27}$	$7.1 \cdot 10^{27}$
SB	3456	1.5	1.7	1.6	1.0	$2.9 \cdot 10^{28}$	$1.7 \cdot 10^{28}$
1F	1296	4.2	4.2	2.3	2.5	$4.2 \cdot 10^{28}$	$4.9 \cdot 10^{28}$
1N	2340	4.4	4.2	2.7	2.5	$1.2 \cdot 10^{29}$	$1.1 \cdot 10^{29}$
1B	1586	4.7	4.2	3.2	2.5	$5.0 \cdot 10^{29}$	$3.5 \cdot 10^{29}$
2F	59	9.9	11.9	3.3	5.2	$3.2 \cdot 10^{29}$	$6.2 \cdot 10^{29}$
2N	268	10.3	11.9	4.4	5.2	$1.5 \cdot 10^{30}$	$2.0 \cdot 10^{30}$
2B	453	10.8	11.9	5.0	5.2	$5.9 \cdot 10^{30}$	$6.2 \cdot 10^{30}$
3F	6	27.2	24.6	3.5	8.8	$2.8 \cdot 10^{30}$	$7.1 \cdot 10^{30}$
3N	11	22.7	24.6	9.1	8.8	$2.2 \cdot 10^{31}$	$2.2 \cdot 10^{31}$
3B	48	25.0	24.6	6.6	8.8	$4.4 \cdot 10^{31}$	$6.0 \cdot 10^{31}$
4F	0	–	42.5	–	13.0	–	$5.5 \cdot 10^{31}$
4N	2	37.9	42.5	2.7	13.0	$2.8 \cdot 10^{31}$	$1.5 \cdot 10^{32}$
4B	3	48.1	42.5	3.7	13.0	$1.3 \cdot 10^{32}$	$4.5 \cdot 10^{32}$

Notes: Column I – results of this work; Column II – data from [Kurochrka, Stasjuk, 1981; Kurochka, Rossada, 1981a, 1981b].

They, however, show that between optical flares of different area classes there is a significant mutual overlap in energies (Figure 10. *a*, *b*; Table 8).

Up to 9.5 % of small flares (class S) fall within the energy range of large solar flares (classes 2–4). A more considerable overlap is with class 1 flares. Note that flares with super-long lifetimes are omitted in this case [Borovik, Zhdanov, 2018a].

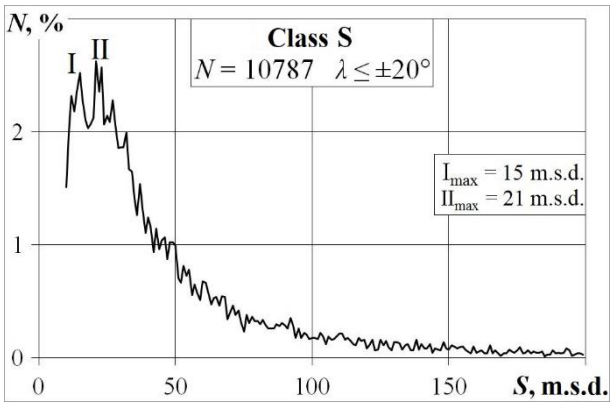

Figure 9. Area distribution of small flares within 20° from the central meridian as derived from HOLL, LEAR, and RAMY data

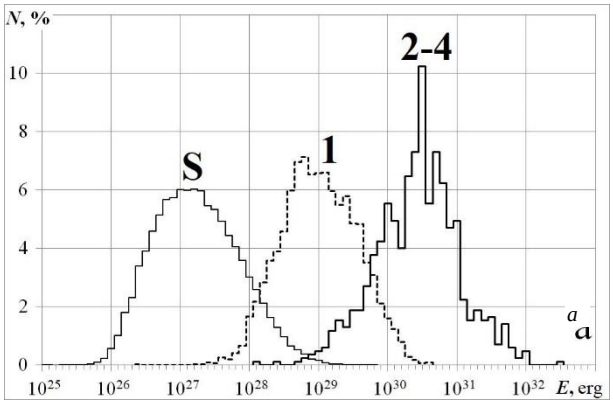

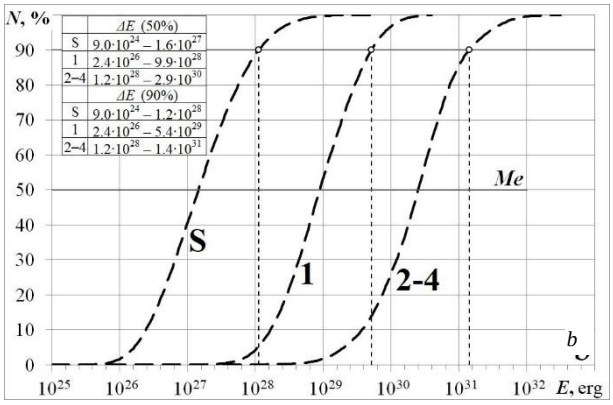

Figure 10. Distribution of solar flares by energy (*a*); cumulative frequency plots (*b*)

Table 8

Statistical parameters of distributions of flares by energies. L is the distribution range

	N	$\bar{E} \pm \alpha$	Me	ΔE (90 %)	L
S	68688	$5.1 \cdot 10^{27} \pm 0.09$	$1.6 \cdot 10^{27}$	$9.0 \cdot 10^{24}$ – $1.2 \cdot 10^{28}$	$9.0 \cdot 10^{24}$ – $5.9 \cdot 10^{29}$
1	5222	$2.2 \cdot 10^{29} \pm 0.09$	$9.9 \cdot 10^{28}$	$2.4 \cdot 10^{26}$ – $15.4 \cdot 10^{29}$	$2.4 \cdot 10^{26}$ – $4.2 \cdot 10^{30}$
2–4	850	$7.0 \cdot 10^{30} \pm 1.10$	$2.9 \cdot 10^{30}$	$1.2 \cdot 10^{28}$ – $1.4 \cdot 10^{31}$	$1.2 \cdot 10^{28}$ – $3.3 \cdot 10^{32}$

CONCLUSIONS

The results of the study allow us to draw the following conclusions:

•Using extensive statistical data on small solar flares, we have established a high correlation between brightness rise time and total duration of flares.

• We have obtained new data on the mean relative brightness rise time of solar flares for different area classes, importance, and brightness. We have shown that with increasing area class, importance, and brightness the mean relative brightness rise time decreases.

• We have found that small flares with one brilliant point and spotless flares have the longest relative brightness rise times. Small explosive flares and two-ribbon flares have the shortest brightness rise times.

• We have found evidence of possible discreteness of T_{rel} for small solar flares — a series of maxima on the distribution of T_{rel}. The most significant of them are 0.2, 0.25, 0.33, and 0.5. With increasing importance and area class of flares, the maxima decrease, flatten, and disappear completely in case of large flares. There are identical maxima in distributions of small D-flares and G-flares. On distributions of V-, H-, and E-flares, they gradually decrease and disappear in U- and K-flares.

• We have obtained the distribution of solar flares by energy in the optical wavelength range, which indicates that there is a significant overlap in energies between flares of different area classes. Up to 9.5 % of small flares (class S) fall within the energy range of large solar flares (classes 2–4). A more considerable overlap is with class 1 flares.

The work was performed with budgetary funding of Basic Research program II.16 No. 1.6.

REFERENCES

Borovik A.V. Solar flares and supergranulation structure of active regions. *Issledovaniya po geomagnetizmu, aeronomii i fizike Solntsa* [Res. on geomagnetism, Aeronomy and Solar Phys.]. 1990, iss. 91, pp. 141–144. (In Russian).

Borovik A.V. Statistical parameters and fine structure elements of small solar flares. *Issledovaniya po geomagnetizmu, aeronomii i fizike Solntsa* [Res. on geomagnetism, Aeronomy and Solar Phys.]. 1994, iss. 102, pp. 161–177. (In Russian).

Borovik A.V., Zhdanov A.A. Statistical studies of low-power solar flares. Distribution of flares by area, brightness, and classes. *Solar-Terr. Phys*. 2017a, vol. 3, no. 1, pp. 40–56. DOI: 10.12737/article_58f96fda7e3e76.83058648.

Borovik A.V., Zhdanov A.A. Statistical research into low-power solar flares. Main phase duration. *Solar-Terr. Phys*. 2017b, vol. 3, no. 4. P. 5–16. DOI: 10.12737/stp-34201701.

Borovik A.V., Zhdanov A.A. Statistical studies of duration of low-power solar flares. *Solar-Terr. Phys*. 2018a. vol. 4, no. 2, pp. 8–16. DOI: 10.12737/stp-42201803.

Borovik A.V., Zhdanov A.A. Distribution of low-power solar flares by brightness rise time. *Solar-Terr. Phys*. 2018b, vol. 4, no. 3, pp. 3–12. DOI: 10.12737/stp-43201801.

Fletcher L., Dennis B.R., Hudson H.S., Krucker S., Phillips K., Veronig A., et al. An observational overview of solar flares. *Space Sci. Rev*. 2011, vol. 159, pp. 19–106. DOI: 10.1007/s11214-010-9701-8.

Kurochka L.N., Rossada V.M. Radiation energy of optical solar flares, II. Solnechnye dannye [Solar Data]. 1981a, no. 6, pp. 78–83. (In Russian).

Kurochka L.N., Rossada V.M. Radiation energy of optical solar flares, III. Solnechnye dannye [Solar Data]. 1981b, no. 7, pp. 95–104. (In Russian).

Kurochka L.N., Stasjuk L.A. Radiation energy of optical solar flares, I. *Solnechnye dannye* [Solar Data]. 1981, no. 5, pp. 83–91. (In Russian).

Masuda S., Kosugi T., Hara H., Tsuneta S., Ogawara Y. Loop-top impulsive hard X-ray source of a solar flare as evidence for magnetic reconnection. *Nature*. 1994, vol. 371, pp. 495–497. DOI: 10.1038/371495a0.

Neupert W.M. Comparison of solar X-ray line emission with microwave emission during flares. *The Astrophys. J*. 1968, vol. 153, pp. L59–L64. DOI: 10.1086/180220.

Ogir' M.B. Some types of movements in chromospheric flares. *Izvestija Krymskoi astrofizicheskoi observatorii* [Bull. of the Crimean Astrophysical Observatory]. 1970, vol. 16–17, pp. 25–44. (In Russian).

Priest E. *Solnechnaya magnitogidrodinamika* [Solar Magnetohydrodynamics]. Moscow, Mir Publ., 1985, 592 p. (In Russian).

Priest E.R. Solar flare MHD processes. *Pub. Astron. Inst. Acad. Sci. Czech. Republic*. 1992, vol. 88, pp. 95–120.

Raman S.K., Aleem S.M., Singh J., Selvendran R., Thiagarajan R. H-alpha flare of 14 March, 1984 − Evidence for reconnection? *Solar Phys*. 1994, vol. 149, no. 1, pp. 119–127. DOI: 10.1007/BF00645182.

Roumeliotis G., Moore RL A linear solution for magnetic reconnection by converging or diverging footpointmotions. *The Astrophys. J*. 1993, vol. 416, no. 1, pt. 1, pp. 386–391. DOI: 10.1086/173243.

Rust D.M., Gauzzi G. Variation of the vector magnetic field in an eruptive flare // World Space Congress: the 43rd Congress of the International Astronautical Federation (IAF) and the 29th Plenary Meeting of the Committee of Space Research (COSPAR). Washington. 1992. P. 486.

Severnyi A.B., Shaposhnikova E.F. Dynamics of limb flares on the Sun and pinch effect. *Izvestija Krymskoi astrofizicheskoi observatorii* [Bull. of the Crimean Astrophysical Observatory]. 1961, vol. 24, pp. 235–257. (In Russian).

Smith H., Smith E. *Solnechnye vspyshki* [Solar Flares] Moscow, Mir Publ., 1966, 426 p. (In Russian). English edition: Smith H.J., Smith E. Solar Flares. Macmillan, 1963. 322 p.

Solar Geophys. Data. 1983. Pt. 1, January, N 461. P. 30.

Somov B.V. Physical Processes in Solar Flares. Dordrecht; Boston: Kluwer Academic Publ. 1992. 249 p.

Švestka Z. Solar flares. Dordrecht: Reidel, 1976. 399 p.

Woods T.N., Kopp G., Chamberlin P.C. Contributions of the solar ultraviolet irradiance to the total solar irradiance during large flares. *J. Geophys. Res.* 2006, vol. 111, iss. A10, pp. 1–10. DOI: 10.1029/2005JA011507.

How to cite this article

Borovik A.V., Zhdanov A.A. Processes of energy release in low-power solar flares. *Solar-Terrestrial Physics*. 2019. Vol. 5. Iss. 4. P. 3–9. DOI: 10.12737/stp-54201901.